Journal of
**Synchrotron
Radiation**

ISSN 0909-0495

Received 20 December 2012
Accepted 16 May 2013

VUV photochemistry simulation of planetary upper atmosphere using synchrotron radiation

Nathalie Carrasco,[a]* Alexandre Giuliani,[b,c]* Jean-Jacques Correia[a] and Guy Cernogora[a]

[a]Université de Versailles St-Quentin/UPMC Université Paris 06, CNRS, LATMOS, F-78280 Guyancourt, France, [b]Synchrotron SOLEIL, L'Orme des Merisiers, Saint-Aubin, BP 48, F-91192 Gif-sur-Yvette, France, and [c]UAR1008 CEPIA, INRA, Rue de la Geraudiere, F-44316 Nantes, France. E-mail: nathalie.carrasco@latmos.ipsl.fr, alexandre.giuliani@synchrotron-soleil.fr

The coupling of a gas reactor, named APSIS, with a vacuum-ultraviolet (VUV) beamline at the SOLEIL synchrotron radiation facility, for a photochemistry study of gas mixtures, is reported. The reactor may be irradiated windowless with gas pressures up to hundreds of millibar, and thus allows the effect of energetic photons below 100 nm wavelength to be studied on possibly dense media. This set-up is perfectly suited to atmospheric photochemistry investigations, as illustrated by a preliminary report of a simulation of the upper atmospheric photochemistry of Titan, the largest satellite of Saturn. Titan's atmosphere is mainly composed of molecular nitrogen and methane. Solar VUV irradiation with wavelengths no longer than 100 nm on the top of the atmosphere enables the dissociation and ionization of nitrogen, involving a nitrogen chemistry specific to nitrogen-rich upper atmospheres.

Keywords: atmosphere; reactivity; VUV photochemistry; planets; Titan.

1. Introduction

Synchrotron radiation has been used for studying photochemical processes in dedicated beamlines (Takahashi *et al.*, 1998) and endstations (Pantförder *et al.*, 2005; Kennepohl *et al.*, 2009); most of these studies involved X-rays and reduced pressures, up to the millibar range (Pantförder *et al.*, 2005).

Vacuum-ultraviolet (VUV) is the wavelength range of greatest interest in simulations of atmospheric photochemistry triggered by sunlight. Synchrotron radiation is an extremely useful tool for accessing this wavelength range and its spectrum overlaps the solar spectrum perfectly (Pilling *et al.*, 2009). Indeed, comparison of the solar flux with the energy-integrated photon flux delivered by beamlines has allowed some authors (Pilling *et al.*, 2009) to estimate that a 1 h white-beam irradiation process corresponds to 10^5 years of solar soft-X ray exposure on the basis of a comparison of the integrated photon fluxes. Surprisingly, synchrotron radiation in the VUV range has not frequently been used in this respect.

This pertains to two usually incompatible requirements: the VUV irradiation condition and a strong pressure gradient between the reactor and the synchrotron beamline. Fluoride windows are often used to confine the gas mixture in the reaction vessel. This situation occurs often in simulations based on laboratory Lyman-α sources (Ádámkovics & Boering, 2003; Trainer *et al.*, 2004; Romanzin *et al.*, 2008), but with the drawback of cutting off the shorter-wavelength radiation. If the higher energy part of the spectrum is required, then it is mandatory to work windowless, since vacuum-tight windows made of LiF, CaF_2 or MgF_2, for example, are opaque to VUV below 100 nm, a wavelength range mandatory to enable molecular nitrogen dissociation (see Fig. 1).

Under these experimental conditions the maximum pressure reachable in the reaction chamber is limited by the efficiency of the differential pumping that accommodates the pressure difference between the chamber and the beamline. This explains the recent efforts made in the development of differential pumping systems to deliver radiation at higher pressures, up to the bar range (Gog *et al.*, 2007; Tamenori, 2010; Giuliani *et al.*, 2011). The DISCO beamline at SOLEIL (Giuliani *et al.*, 2009), a bending-magnet-based VUV beamline, possesses a branch, referred to as the Atmospheric Pressure EXperiment (APEX) branch, fitted with a differential pump that works with rare gases up to 1 bar (Giuliani *et al.*, 2011). Fig. 1 compares the photon flux of the APEX branch at the position of the reactor with that of the sun and also provides the photoabsorption cross section for methane and nitrogen. It clearly shows that wavelengths below 100 nm are required to simulate the partial dissociation and ionization occurring in nitrogen-rich planetary upper atmospheres. This is especially the case for the atmosphere of Titan, the largest

doi:10.1107/S0909049513013538

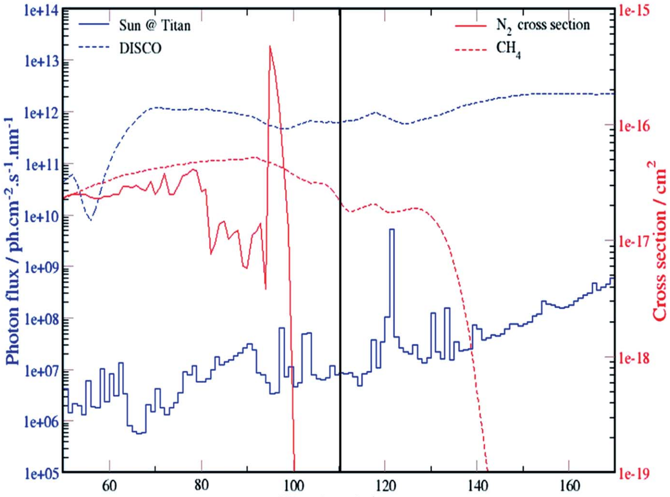

Figure 1
DISCO energy spectrum in the APEX branch at the entrance of the APSIS set-up (blue dashed line) and solar spectrum at the top of Titan's atmosphere (blue full line). Photoabsorption cross sections of methane (red dashed line) and molecular nitrogen (red full line) [adapted from Gans *et al.* (2013)]. The transparency limit of the fluoride windows is indicated by the vertical line at 110 nm.

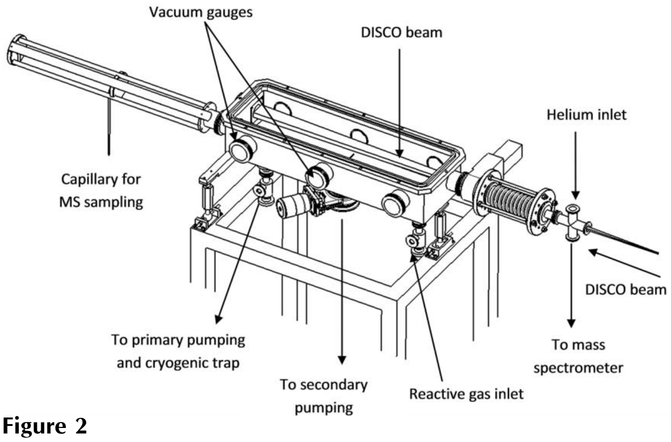

Figure 2
Schematic diagram of the APSIS set-up.

satellite of Saturn, in which an intense chemistry leads to the production of aerosols rich in nitrogen and carbon in the ionosphere (Israel *et al.*, 2005; Waite Jr *et al.*, 2007).

We report here on a new gas reactor, named APSIS (Atmospheric Photochemistry SImulated by Synchrotron), mounted on the APEX branch of the DISCO beamline at SOLEIL. The reactor allows a wide range of photochemical processes to be studied, ranging from those occurring in the upper part of the atmosphere to those taking place in lower parts, such as the Earth's troposphere, using a single instrument working in the range from 10^{-4} mbar up to 10^3 mbar over the 350–55 nm wavelength region. The characteristics of the reactor are discussed first, followed by a preliminary application to a simulation of Titan's upper atmosphere.

2. Experimental set-up

2.1. The APSIS reactor

The reactor, represented in Fig. 2, is made of a stainless steel chamber bearing a gas inlet from which the reactive mixture is introduced. The gas mixture flow rate admitted in the reactor is controlled by a gas flow controller (10 sccm full scale; MKS mass flow controller; sccm = standard cubic centimetres per minute), and the pressure under working conditions is measured by a capacitance gauge (10 mbar full scale; MKS baratron). The pressure appeared to be very stable in the reactor; no variation could be detected within the precision of the gauge (0.25% full scale). The gas flow is maintained by a primary pump (Edwards XDS 10) during irradiation. In the present configuration, neutral molecules formed upon irradiation are detected by a quadrupole mass spectrometer (Pfeiffer QME 200), which is connected to the reaction chamber by a moveable nose. The system could also be used in another configuration in which the ion population will be measured. This kind of information will be totally complementary to the detection of the neutrals. The reactor is evacuated by a turbomolecular pump (Pfeiffer HiPace 80) prior to the introduction of the mixture, down to 10^{-5} mbar measured by a cold cathode gauge. The pressure and then the time of residence of the gases inside the reactor for a given gas flow rate may be controlled by the adjustment of the primary pumping flow.

A four-ways cross pipe is added in front of the reactor, between the entrance of the reactor and the differential pumping of the synchrotron branch line (see Fig. 2). This gas inlet enables a flow of a non-reactive rare gas, such as helium, to be introduced which confines the reactive gas mixture in the APSIS reactor, without modifying the chemistry in the reactor. This prevents pumping the reactive mixture in the first stages of the differential pumping and thus the photochemistry to occur outside of the reactor. The absence of reactant gases flowing out of the reactor to the beamline is checked by sampling the nature of the gases using the mass spectrometer on the four-ways cross pipe. The helium flow limits the higher photon energy delivered to the reactor up to its ionization threshold at 24.58 eV (Rosenstock *et al.*, 2011). Other curtain gases may be used, such as neon or krypton, to narrow even more the photon energy window.

Once the gas flow is steadily established, a background mass spectrum is recorded without irradiation, which establishes the reference for consumption or production of the molecular species.

3. Application: simulation of Titan's upper atmosphere

Titan is the largest satellite of Saturn, with a dense atmosphere of 1.5 bar at the planet surface mainly composed of nitrogen and methane. An intense atmospheric chemistry leads to the production of aerosols rich in nitrogen and carbon up to the ionosphere (Israel *et al.*, 2005; Waite Jr *et al.*, 2007). VUV photochemistry occurs in Titan's stratosphere and above: methane photolysis at 140 nm is shown to be efficient at 400 km height for example (Gans *et al.*, 2013), where the pressure is a few 10^{-1} mbar.

Previous simulations of Titan's upper atmosphere using synchrotron radiation have been reported. Pilling *et al.* (2009) studied the production of analogs of Titan's aerosols by X-ray irradiation on a condensed film of N_2–CH_4 at 14 K. Thissen *et al.* (2009) studied the ions produced after irradiating Titan-like gas mixtures by VUV in an ion-cyclotron-resonance mass spectrometer cell. The very low pressure of 10^{-8} mbar was in this case well representative of Titan's ionosphere at ~1000 km, but the small size of the cell (8 cm^3) was inappropriate for studying sequences of reactions between reactive gas species, and the authors observed an important contribution from wall effects. This experience illustrates the difficulty in the laboratory to simulate the atmospheric photochemical processes under lower-pressure conditions, without prominent wall effects. The mean free path of the reactant species has to be several orders of magnitudes lower than the smallest dimension of the reactor. For instance, Imanaka & Smith (2007) developed a 1 m-length photochemical reactor to be coupled with a VUV synchrotron beamline and irradiated a N_2–CH_4 gas mixture at ~10^{-1} mbar at 60 nm and 85 nm wavelength to probe the effect of N_2 ionization on the chemical growth.

Here, a mixture composed of 90% nitrogen and 10% methane has been introduced at a 10 sccm flow rate in the reactor along with helium giving a partial N_2–CH_4 pressure of 6 mbar and an overall pressure of 9 mbar. The monochromator of the beamline was set to the zero order (*i.e* the grating acts as a mirror) in order to send the full white beam on the reactive mixture. The time-dependent evolution of the gas mixture composition was monitored by recording the intensity of the maximum of mass peaks of interest in multiple ion detection (MID) mode: m/z = 15, 26, 27, 28, 38, 39, 41 and 52. Except for m/z = 15 [methane fragment signature (Sciamma-O'Brien *et al.*, 2010)] and 28 (nitrogen signature), the ion masses chosen in the MID method correspond to product formation in mass regions X_2, X_3 and X_4, with two, three or four heavy (C or N) atoms bearing species, respectively. The relative consumption of methane is about 10^{-3} after ~5 min of DISCO irradiation. The DISCO photon flux (a few 10^{11} photons s^{-1} at 100 nm for 0.1 nm bandwidth) leads to a nitrogen dissociation ratio of less than 10^{-4}. The signal at m/z = 28 of N_2 should therefore be constant enough throughout the experiments to be considered as a fixed reference. The intensity of the mass peak at m/z = 28 is therefore used to normalize the mass spectra.

Species with mass signatures at m/z = 26, 27, 38, 39, 41 and 52 are produced (see Fig. 3), showing a production of X_2, X_3 and X_4 species. Even if the MS peak intensities are not directly representative of the corresponding neutral concentrations owing to the different ionization thresholds and fragmentation patterns of the products, the ratio of the main peaks intensities against the one at m/z = 28 provides a rough estimation of the mole fraction of the products diluted in N_2. Products mole fractions are about 10^{-5} for X_2 compounds and around the p.p.m. for X_3 and X_4 species.

Moreover, peaks at m/z = 27, 41 and 52 are the major ions in their respective X_2, X_3 and X_4 m/z domains, corresponding to parent ions of neutral products. Odd masses are distinctive of nitrogen-bearing ions. They correspond therefore to the parent ions of the nitrogen-bearing molecular species HCN, CH_3CN and C_2N_2, respectively. The identification has moreover been confirmed by a chemical gas-chromatography–mass-spectrometry analysis of the gas phase (Peng *et al.*, 2013). This confirms the direct molecular nitrogen reactivity under the VUV DISCO irradiation conditions, as observed in Titan's upper atmosphere.

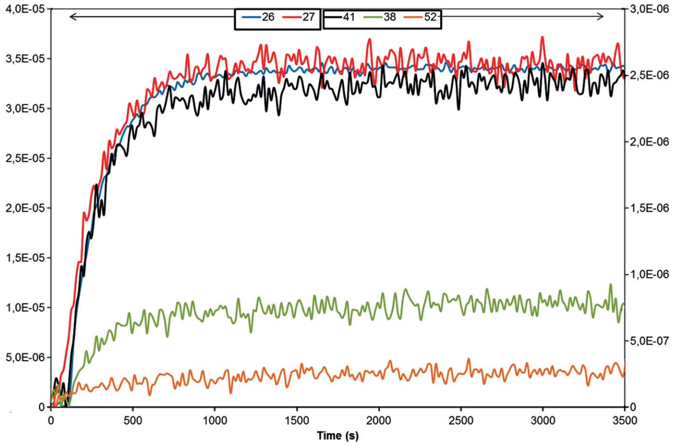

Figure 3
Time monitoring of products. The time origin corresponds to the beginning of the irradiation. Relative concentrations of m/z = 26 and 27 (relatively to N_2, m/z = 28 intensity) are reported on the left-hand *y* axis, whereas m/z = 41, 38 and 52 are reported on the right-hand *y* axis.

4. Conclusion

We report here the first results from the coupling of a VUV synchrotron beamline with a windowless gas reactor, named APSIS, able to simulate various kinds of atmospheric composition and pressure. We used a nitrogen–methane gas flow mixture, similar to that found on Titan, which was irradiated by a continuous 60–350 nm VUV beam provided by the DISCO beamline at the SOLEIL synchrotron radiation facility. The feasibility of atmospheric photochemistry simulations has been demonstrated in this study, showing the great potential of this platform for further investigations of planetary atmospheres.

The conception and construction of the APSIS reactor was supported by the CNES (Centre National d'Etude Spatiale) and the PRES UniverSud Paris. Experiments were performed on the DISCO beamline at the SOLEIL synchrotron, France, under proposal numbers 20100104 and 20100723. We are grateful to the SOLEIL staff for smoothly running the facility.

References

Ádámkovics, M. & Boering, K. A. (2003). *J. Geophys. Res.* **108**, 5092.

Gans, B., Peng, Z., Carrasco, N., Gauyacq, D., Lebonnois, S. & Pernot, P. (2013). *Icarus*, **223**, 330–343.

Giuliani, A., Jamme, F., Rouam, V., Wien, F., Giorgetta, J.-L., Lagarde, B., Chubar, O., Bac, S., Yao, I., Rey, S., Herbeaux, C., Marlats, J.-L., Zerbib, D., Polack, F. & Réfrégiers, M. (2009). *J. Synchrotron Rad.* **16**, 835–841.

Giuliani, A., Yao, I., Lagarde, B., Rey, S., Duval, J.-P., Rommeluere, P., Jamme, F., Rouam, V., Wein, F., De Oliveira, C., Ros, M., Lestrade, A., Desjardins, K., Giorgetta, J.-L., Laprevote, O., Herbaux, C. & Refregiers, M. (2011). *J. Synchrotron Rad.* **18**, 546–549.

Gog, T., Casa, D. M., Kuzmenko, I., Krakora, R. J. & Bolin, T. B. (2007). *J. Synchrotron Rad.* **14**, 339–344.

Imanaka, H. & Smith, M. A. (2007). *Geophys. Res. Lett.* **34**, L02204.

Israel, G., Szopa, C., Raulin, F., Cabane, M., Niemann, H. B., Atreya, S. K., Bauer, S. J., Brun, J. F., Chassefiere, E., Collect, P., Conde, E., Coscia, D., Hauchecorne, A., Millian, P., Nguyen, M. J., Owen, T., Riedler, W., Samuelson, R. E., Siguier, J. M., Steller, M., Sternberg, R. & Vidal-Madjar, C. (2005). *Nature (London)*, **438**, 796–799.

Kennepohl, P., Wasinger, E. C. & DeBeer George, S. (2009). *J. Synchrotron Rad.* **16**, 484–488.

Pantförder, J., Pöllmann, S., Zhu, J. F., Borgmann, D., Denecke, R. & Steinrück, H. (2005). *Rev. Sci. Instrum.* **76**, 014102.

Peng, Z., Gautier, T., Carrasco, N., Pernot, P., Giuliani, A., Mahjoub, A., Correia, J.-J., Buch, A., Bénilan, Y., Szopa, C. & Cernogora, G. (2013). *J. Geophys. Res.* **118**, 1–11.

Pilling, S., Andrade, D. P., Neto, A. C., Rittner, R. & Naves de Brito, A. (2009). *J. Phys. Chem. A*, **113**, 11161–11166.

Romanzin, C., Bénilan, Y., Jolly, A. & Gazeau, M. C. (2008). *Adv. Space Res.* **42**, 2036–2044.

Rosenstock, H. M., Draxl, K. & Steiner, B. W. (2011). *Ion Energetics Data.* In *NIST Chemistry WebBook.* NIST Standard Reference Database Number 69, National Institute of Standards and Technology, Gaithersburg, MD 20899, USA.

Sciamma-O'Brien, E., Carrasco, N., Szopa, C., Buch, A. & Cernogora, G. (2010). *Icarus*, **209**, 704–714.

Takahashi, J., Utsumi, Y., Hosokawa, T., Ushiki, J. & Tadano, T. (1998). *J. Synchrotron Rad.* **5**, 548–550.

Tamenori, Y. (2010). *J. Synchrotron Rad.* **17**, 243–249.

Thissen, R., Vuitton, V., Lavvas, P., Lemaire, J., Dehon, C., Dutuit, O., Smith, M. A., Turchini, S., Catone, D., Yelle, R. V., Pernot, P., Somogyi, A. & Coreno, M. (2009). *J. Phys. Chem. A*, **113**, 11211–11220.

Trainer, M. G., Pavlov, A. A., Curtis, D. B., McKay, C. P., Worsnop, D., Delia, A. E., Toohey, D. W., Toon, O. B. & Tolbert, M. A. (2004). *Astrobiology*, **4**, 409–419.

Waite, J. H. Jr, Young, D. T., Cravens, T. E., Coates, A. J., Crary, F. J., Magee, B. & Westlake, J. (2007). *Science*, **316**, 870–875.